

Title Page

Title: Diffusion kurtosis imaging combined with dynamic susceptibility contrast-enhanced MRI in differentiating high-grade glioma recurrence from pseudoprogression

Manuscript Type: Original Research.

Author names and affiliations:

Wenwei Shi^{1#} (MD), Chongxiao Qu^{2#} (MD), Xiaochun Wang³ (MD), Xiao Liang⁴ (MD), Yan Tan^{3*} (MD), Hui Zhang^{3*} (MD)

1 Department of Radiology, Zhongda Hospital, Southeast University, No.87 Dingjiaqiao, Nanjing 210009, Jiangsu Province, P.R. China (W.S.)

2 Department of Pathology, Shanxi Provincial People's Hospital Affiliated to Shanxi Medical University, NO.29 of Twin Towers Temple Street, Taiyuan 030012, Shanxi Province, P.R. China (C.Q.)

3 Department of Radiology, First Clinical Medical College, Shanxi Medical University, NO.85 Jiefang South Road, Taiyuan 030001, Shanxi Province, P.R. China (X.W., Y.T., H.Z.)

4 Department of Radiology, Shanxi Provincial People's Hospital Affiliated to Shanxi Medical University, NO.29 of Twin Towers Temple Street, Taiyuan 030012, Shanxi Province, P.R. China (X.L.)

Wenwei Shi and Chongxiao Qu contributed equally to this work.

*** Corresponding author:**

***Hui Zhang**, Department of Radiology, First Clinical Medical College, Shanxi Medical University, NO.85 Jiefang South Road, Taiyuan 030001, Shanxi Province, P.R. China. **E-mail:** zhanghui_mr@163.com. **Tel:** +86-18635580000. **Fax:** +86 351 2024239.

***Yan Tan**, Department of Radiology, First Clinical Medical College, Shanxi Medical University, NO.85 Jiefang South Road, Taiyuan 030001, Shanxi Province, P.R. China. **E-mail:** tanyan123456@sina.com. **Tel:** +86-18636803827. **Fax:** +86 351 4639362.

Diffusion kurtosis imaging combined with dynamic susceptibility contrast-enhanced MRI in differentiating high-grade glioma recurrence from pseudoprogression

Abstract

Objectives: To compare the added value of diffusion kurtosis imaging (DKI) with the combination of dynamic susceptibility contrast-enhanced (DSC) MRI in differentiating glioma recurrence from pseudoprogression.

Methods: Thirty-four patients with high-grade gliomas developing new and/or increasing enhanced lesions within six months after surgery and chemoradiotherapy were retrospectively analyzed. All patients were pathologically confirmed to have recurrent glioma ($n = 22$) or pseudoprogression ($n = 12$). The DKI and DSC MRI parameters were calculated based on the enhanced lesions on contrast-enhanced T1WI. ROC analysis was performed on significant variables to determine their diagnostic performance. Multivariate logistic regression was used to determine the best prediction model for discrimination.

Results: The relative mean kurtosis (rMK), relative axial kurtosis (rKa), relative cerebral blood volume (rCBV), and relative mean transit time (rMTT) of glioma recurrence were higher than those of pseudoprogression (all, $P < 0.05$). The AUCs and diagnostic accuracy were 0.879 and 82.35% for rMK, 0.723 and 70.59% for rKa, 0.890 and 82.35% for rCBV, 0.765 and 73.53% for rMTT, respectively. A multivariate logistic regression model showed a significant contribution of rMK ($P = 0.006$) and rCBV ($P = 0.009$) as independent imaging classifiers for discrimination. The combined

use of rMK and rCBV improved the AUC to 0.924 ($P < 0.001$) and the diagnostic accuracy to 88.24%.

Conclusion: DKI may be a valuable non-invasive tool in differentiating glioma recurrence from pseudoprogression, and its use in combination with DSC MRI can improve diagnostic performance in assessing treatment response compared with either technique alone.

Key words: Glioma; Recurrence; Pseudoprogression; Diffusion kurtosis imaging (DKI); Dynamic susceptibility contrast-enhanced (DSC) MRI

Abbreviations:

DKI = diffusion kurtosis imaging

DSC = dynamic susceptibility contrast-enhanced

TMZ = temozolomide

rMK = relative mean kurtosis

rKa = relative axial kurtosis

rCBV = relative cerebral blood volume

rMTT = relative mean transit time

rADC = relative apparent diffusion coefficient

AUC = area under the receiver operating characteristic curve

Introduction

Gliomas are the most common primary malignant tumors of the central nervous system [1]. The current standard of care for high-grade gliomas (WHO III-IV) consists of neurosurgical excision, followed by radiotherapy and concomitant adjuvant temozolomide (TMZ) chemotherapy [2]. Response assessment in glioma is challenging due to frequent changes in early imaging, especially during the initial six months after chemoradiotherapy. Increased contrast enhancement of lesions occurs at conventional MRI follow-up that could be either recurrent tumor or pseudoprogression because the imaging features of the two overlap to a certain extent [3]. Currently, it is recognized that chemoradiotherapy leads to approximately 33% incidence of pseudoprogression in treated high-grade glioma [4], in which lesions tend to decrease in size or stabilize without further treatment, resulting in longer survival. Recurrent glioma has a poor prognosis and may require repeated surgery due to its rapid progression. Making this distinction correctly is thus essential to the success of a particular treatment and subsequent clinical management.

There are pathophysiologic differences between glioma recurrence and pseudoprogression. Recent advances in MR techniques have made it possible to monitor tumors at the metabolic and microvascular levels. Relative cerebral blood volume (rCBV) derived from dynamic susceptibility contrast-enhanced (DSC) MRI, which is a recognized imaging biomarker of angiogenesis, is the most powerful single imaging classifier and convincing parameter for differentiating glioma recurrence from pseudoprogression [5, 6]. Cerebral blood volume (CBV), a parameter that showed a

reliable correlation with histopathologic findings of neoangiogenesis, can help measure changes related to neovascularization, which is associated with tumor malignancy [7]. Studies have concluded that rCBV, as a single imaging classifier to predict recurrent tumor, was significantly higher than that in patients with pseudoprogression [8]. However, because the optimal reported thresholds vary significantly across institutions [8], and its high sensitivity to magnetic field inhomogeneities or when administration of contrast agent is unavailable, some additional complementary imaging techniques may be help in clinical practice.

Apparent diffusion coefficient (ADC) is a very accessible parameter of diffusion-weighted imaging (DWI), which is often discussed in previous studies. Due to the heterogeneity of recurrent tumors, the reliable evidence of DWI based on Gaussian distribution of water molecules may be limited [9]. Diffusion kurtosis imaging (DKI), a non-invasive tool, is a straightforward extension of DWI that can depict the non-Gaussian diffusion of water molecules and accurately characterize cellular density and tissue heterogeneity information [9]. DKI parameters have recently been utilized as potential imaging biomarkers to grade gliomas and predict its genotype [10-12]. Recent studies have shown that DKI may be a reliable tool in differentiating glioma recurrence from pseudoprogression [13, 14]. However, DKI and DSC techniques have been examined in patients with suspected treatment-related changes individually. To date, there are no reports concerning the utility of combining DKI and DSC techniques. We hypothesized that a combination of DKI and DSC MRI parameters can improve accuracy in making this differentiation. The purpose of the present study was to analyze the added value of DKI with the combination of DSC MRI in discriminating glioma recurrence from pseudoprogression compared with single use.

Materials and methods

Patients

This retrospective study was conducted from August 2017 to August 2019 and approved by the Institutional Ethics Committee of XXX, and informed consent was obtained from all of the study participants. Fifty-three patients met the following inclusion criteria: histopathologically confirmed high-grade gliomas (WHO III-IV) who developed new and/or increasing enhanced lesions after surgery and concurrent chemoradiotherapy within six months, followed up by DKI and DSC MRI, and were assigned to either the recurrence or pseudoprogression group according to the histopathological results of repeat surgery or biopsy. The exclusion criteria were: they did not undergo primary total resection ($n = 8$), they received non-TMZ chemotherapy ($n = 4$), or their follow-up MRI was not available for analysis ($n = 7$ [severe motion artifacts or hemorrhage, $n = 4$; more than 6 months between surgery and follow-up MRI, $n = 3$]). Ultimately, 34 patients were included in the study.

MRI Data Acquisition

All of the image acquisition was performed on a 3.0T MRI scanner (MAGNETOM Skyra, Siemens Healthcare, Erlangen) with a 20-channel array coil. The scanning protocol included transverse T1-weighted images (T1WI), T2-weighted images (T2WI), T2 fluid-attenuated inversion recovery (T2FLAIR), contrast-enhanced T1WI (CE-T1WI), DWI, DKI, and DSC sequences. The parameters were as follows: TR/TE, 220/2.46 ms for gradient-echo T1WI and CE-T1WI; TR/TE, 3570/175 ms for T2WI; TR/TE, 8000/103 ms, and TI, 2374 ms for T2FLAIR; thickness, 6.0 mm; FOV, 220 × 220 mm². Gadolinium chelate (Magnevist, Bayer, Leverkusen) at a dose of 0.1 mmol/kg was used as contrast agent. Approximately 40% of contrast volume was administered intravenously for CE-T1WI at a rate of 3 mL/s, followed by a 20-mL

bolus of saline at the same rate.

DWI was performed by using single-shot echo-planar imaging (EPI) with b-values = 0 and 1,000 s/mm². A single-shot EPI sequence was used to obtain the DKI data. The b values were 0, 1,000, and 2,000 s/mm² along with 30 uniformly distributed directions. The parameters were as follows: TR/TE, 4,000/116 ms; FOV, 220 × 220 mm²; matrix, 192 × 192; and thickness, 4.0 mm [15].

Perfusion images were obtained using the DSC technique with a gradient echo-EPI sequence: TR/TE, 1,600/30 ms; FOV, 240 × 240 mm²; matrix, 128 × 128; thickness, 5.0 mm; a total of 30 dynamic frames. The remaining 60% of the contrast agent was injected at a rate of 4 mL/s, followed by 20 mL of saline flush at the same rate [7].

Image Processing

The DWI data and DSC data were transferred to a post-processing workstation (syngo.via, Siemens Healthcare). ADC map were automatically generated by the scanner software using standard method. DSC data were first corrected for motion. The arterial input function was defined in the tissue from the middle cerebral artery contralateral to the enhancing lesion [7, 16]. DSC parameters, including CBV, cerebral blood flow (CBF), mean transit time (MTT), and time to peak (TTP) were obtained after processing. The eddy current distortions and head motion were corrected by global affine transformations for DKI data using FMRIB Software Library (version 6.0, <https://fsl.fmrib.ox.ac.uk/fsl/fslwiki/FSL>). DKI data were processed with Diffusional Kurtosis Estimator (version 2.6, <https://www.nitrc.org/projects/dke/>) to obtain its metrics, including mean kurtosis (MK), axial kurtosis (Ka), radial kurtosis (Kr), mean diffusivity (MD), and fractional anisotropy (FA). DKI parameters were measured by using MRICron software (version 6.6.2013, <http://www.nitrc.org/projects/mricron/>) [14].

ADC map, DSC and DKI parameter maps were co-registered to the axial CE-T1WI, respectively. Conventional MRI sequences were used to visualize the gross features such as cystic change, necrosis, hemorrhage, enhancing lesions, and perilesional edema. Multiple regions of interest (ROIs) were placed manually within the enhanced lesion on CE-T1WI while excluding the necrotic, cystic change and hemorrhages, and automatically marked on ADC, DSC and DKI parameter maps. If multiple enhanced lesions were present, the ROI was placed on the biopsied lesion, and subsequently measured as described above. These ROIs were drawn on the most hyperaemic areas as shown on the color maps (**Figure 1**). Only the ROI that showed the maximum/minimum value for each parameter, has been selected to represent the ADC value, DSC and DKI parameters. The ADC value, DSC and DKI parameters were normalized with a separate ROI drawn in the contralateral normal appearing white matter of the centrum semiovale to compute standardized parameters, i.e., relative ADC (rADC), rCBV, relative cerebral blood flow (rCBF), relative mean transit time (rMTT), and relative time to peak (rTTP), relative mean kurtosis (rMK), relative axial kurtosis (rKa), relative radial kurtosis (rKr), relative mean diffusivity (rMD), and relative fractional anisotropy (rFA).

Two independent radiologists with 15 and 8 years of experience in neuroradiology and blinded to the pathological results performed image analysis. Each parameter value on the enhancing lesion was measured thrice, followed by the calculation of the total mean value of each parameter for each patient.

Statistical Analysis

Statistical analysis was performed using SPSS (version 19.0, IBM) and Medcalc (version 15.2.2, Ostend) software. Clinical characteristics were compared between the two groups using the χ^2 test for categorical data and the t -test for non-categorical

variables. The Shapiro-Wilk test was used to determine whether the non-categorical variables were normally distributed. Inter-group differences between two groups with respect to relative DKI parameters and relative DSC parameters were compared using the Mann-Whitney U test. Receiver operating characteristic (ROC) curves were generated for DKI, DSC and DWI parameters to compute the areas under ROC curve (AUCs), which were used to evaluate the diagnostic relevance of each parameter. Multivariate stepwise logistic regression analysis was performed for variables to determine the best predictor of differentiation between the two groups. Differences with $P < 0.05$ were considered to be a significant difference.

Results

Patients

The clinical characteristics of the patients are summarized in **Table 1**. A total of 34 patients (24 men and 10 women; mean age, 47 years; range: 21 to 70 years) with high-grade gliomas (WHO III-IV, astrocytomas) after completing standard treatment were included for data analysis. Based on pathological results of repeat surgery ($n = 14$, including 14 patients with tumor recurrence) or biopsy ($n = 20$, including 8 patients with tumor recurrence), patients were assigned into one of the two groups, including 12 patients with pseudoprogression (**Figure 2**) and 22 patients with tumor recurrence (**Figure 3**). Patients were typically treated with a total dose of 60 Gy in 2 Gy daily fractions. None of the clinical characteristics, including sex, age, pathological grading, isocitrate dehydrogenase (IDH) mutation, Karnofsky Performance Status score, and radiation dose, were significant predictors of recurrent glioma or pseudoprogression (all, $P > 0.05$).

IDH mutation status

Among them, 27 patients obtained molecular information from the first surgery, of which 10 patients developed pseudoprogression and 17 patients recurred. IDH mutation occurred in 13 (48.1%) of the 27 patients, among which 7 patients developed to pseudoprogression (70% of the 10 cases in the pseudoprogression group), and 6 patients developed to tumor recurrence (35.3% of the 17 cases in the recurrence group). IDH mutations appeared to have a higher probability of pseudoprogression than recurrence, but there was no statistical difference between the two ($P = 0.089$).

DWI, DKI and DSC parameters for the differentiation

rADC values were lower in the glioma recurrence group than in the pseudoprogression group ($P = 0.033$). rMK, rKa, rCBV and rMTT values were higher in the glioma recurrence group than in the pseudoprogression group ($P < 0.001$, $P = 0.033$, $P < 0.001$, $P = 0.012$, respectively). There were no significant differences in rKr, rMD, rFA, rCBF, and rTTP values between glioma recurrence and pseudoprogression (all, $P > 0.05$) (**Table 2**). The box-and-whiskers graphs for the DWI, DKI and DSC parameters are shown in **Figure 4**.

The AUCs of rADC, rMK, rKa, rCBV and rMTT values used to differentiate glioma recurrence from pseudoprogression were 0.723 ($P = 0.041$), 0.879 ($P < 0.001$), 0.723 ($P = 0.030$), 0.890 ($P < 0.001$) and 0.765 ($P = 0.001$), respectively (**Figure 5**). The cut-off value, accuracy, sensitivity, and specificity of rADC, rMK, rKa, rCBV and rMTT are summarized in **Table 3**.

Multivariable analysis to identify the best predictor of the differentiation

For multivariable analysis, we included rMK, rKa, rCBV, rMTT and rADC, and all of the parameters showed significant differences between glioma recurrence and pseudoprogression (all, $P < 0.05$). Multivariable stepwise logistic regression analysis showed that rMK ($P = 0.006$) and rCBV ($P = 0.009$) were significant predictors for

differentiating glioma recurrence from pseudoprogression, whereas rKa ($P = 0.524$), rMTT ($P = 0.556$) and rADC ($P = 0.097$) were not. The combination of rMK and rCBV reached an AUC of 0.924 ($P < 0.001$), an accuracy of 88.24%, a sensitivity of 86.36%, and a specificity of 91.67% (**Table 3**).

Discussion

This study assessed DKI in differentiating recurrent tumors from pseudoprogression, and evaluated the added value of DKI in combination with DSC MRI in this differentiation. Our study showed that rMK can differentiate recurrent tumor from pseudoprogression with high diagnostic accuracy, and its application value alone is similar to that of rCBV. Another finding is that using the combination of DKI and DSC MRI improves diagnostic performance compared to either technique alone.

rMK values were significantly higher in the glioma recurrence group than in the pseudoprogression group, which can be used to distinguish physiological differences between the two groups. As known, MK can reflect the difference of tumor internal heterogeneity, and the greater the parameter value of MK, the more complex the structure [9]. Tumor recurrence was confirmed to be associated with more tumor angiogenesis, greater nuclear atypia, and increased cell density, whereas pseudoprogression is characterized by radiation-induced vascular changes leading to vasodilation, edema, and increased capillary permeability [17]. This results in a more complex structure of recurrent tumor than pseudoprogression, resulting in a higher MK value. Thus, MK is meaningful in terms of classification, consistent with the latest research finding by *Wu et al.* [14]. rKa reflects the integrity of axons and the density of fiber bundles [18], which was slightly higher in recurrent tumor, but most of the 95% confidence interval of the two still overlap. We did not observe differences in another kurtosis parameter, rKr affected by myelin integrity and axonal density [18], which

could be explained by the fact that we focused on only specific regions, i.e., enhanced lesions, rather than analyzing the entire lesion. After chemoradiotherapy, axial rupture and demyelination were observed in both regions to varying degrees, leading to different changes in the above two parameters. Actually, differences in rMD and rFA between the two groups have been controversial [19, 20], partly due to the orientation of extracellular matrix, extent of cellular death, and vascular changes. Changes in MD and FA due to micronecrosis or changes in the viscosity of the medium may offset the decrease or increase in MD or FA in glioma recurrence, resulting in MD and FA values similar to those of pseudoprogression. Studies with larger data sets would be conducted to verify the result. DKI may serve as a novel imaging biomarker for differentiation by characterizing the heterogeneity of the microenvironment.

DKI parameters can be used to evaluate the IDH genotype of astrocytoma, and the MK, Ka and Kr values of IDH-mutant were significantly lower than those of IDH-wild type in the previous study [12]. IDH mutation is associated with pseudoprogression [21]. According to the molecular information, the proportion of IDH-mutant and IDH-wild type in our cases was close, which may be the reason that the 95% confidence interval of DKI parameters was relatively wide and the difference between the recurrence and pseudoprogression groups was not significant.

Our study produced significantly higher rCBV and rMTT values in the recurrence group than in the pseudoprogression group. rCBV was the most accurate parameter in the application of DSC MRI to distinguish between recurrence and pseudoprogression, as in most previous studies [5, 6, 8]. Newly formed immature blood vessels of recurrent tumors can produce increased blood volume, as well as proportions of tumor cells, resulting in significantly higher CBV values [22, 23]. The higher CBV in tumors are associated with poor prognosis after radiotherapy, suggesting that a large number of

tumor-induced angiogenesis are related to more active tumor growth [24]. According to a meta-analysis [8], the threshold of rCBV ranged from 0.9 to 2.15, with pooled sensitivity and specificity of both 88%. In comparison, when we used the mean rCBV, we observed that a threshold of 1.35 led to a sensitivity of 86.36% and specificity of 83.33%.

It is clear that increased contrast enhancement due to a disrupted blood-brain barrier may be affected by several factors, including acute changes after surgery or radiotherapy, chemotherapy, as well as MRI technical issues and administration of gadolinium [25]. ROC analysis showed that both rMK and rCBV demonstrated good classification ability and presented a similar diagnostic accuracy in distinguishing tumor recurrence from pseudoprogression. To our knowledge, there are no studies combined DKI and DSC MRI for distinguishing recurrent tumor and pseudoprogression. Multivariate logistic regression analysis of the imaging parameters indicated that the best classification of tumor recurrence and pseudoprogression was achieved using the rMK and rCBV. The combined use of the two parameters improved the diagnostic performance compared with either technique alone, and is probably related to the fact that changes associated with the treatment of lesions are complex and variable [25]. Therefore, mean rMK and rCBV may be influenced by the parameters from both tumoral and nontumoral components. Multiparametric MRI has recently become a topic of research interest in differentiating glioma recurrence from pseudoprogression [26, 27]. Quantitative analysis of DKI and DSC MRI parameters from the enhanced lesions can be used to assess treatment response in patients with high-grade gliomas, which may contribute to individualized treatment management and better clinical decision-making.

ADC is a simple and easily accessible DWI parameter, has been shown to be

extremely useful in the clinical evaluation of brain tumors. Moreover, ADC values in the recurrent group were significantly lower than those in the pseudoprogression group, which was consistent with the results of previous study [28]. However, its AUC was lower than some of DKI and DSC parameters in our study, and ADC was excluded in the analysis of multivariate logistics regression. The possible reason was that compared with DKI, ADC was a parameter based on the Gaussian motion of water molecules and could not accurately reflect the heterogeneity of tumor recurrence. Despite studies showing that DKI provide largely comparable measures of diffusivity, the longer acquisition times compared with ADC does not seem to provide additional prognostic value [29]. But the complexity of the tissue increases after chemoradiotherapy, ADC may not be a reliable parameter compared with DKI, a technique based on non-Gaussian distribution of water molecules.

The present study has some limitations, including a retrospective analysis design and a relatively small sample size study conducted in a single institution, and the number of tumor types was disproportionate. We use histopathology as the reference standard of imaging results, which may have decreased our evaluation of the combined DKI and DSC model. Further studies with larger sample sizes are needed to confirm our findings. Second, the ROI-based approach has location and/or organizational composition bias. ROI of each lesion was plotted three times to minimize this bias. Third, the longer scanning time of DKI limits its clinical application. The optimal scanning protocol needs to be further explored.

Conclusion

DKI may be a valuable non-invasive tool in differentiating glioma recurrence from pseudoprogression, and its use in combination with DSC MRI can improve diagnostic

performance in assessing treatment response compared with either technique alone.

References

1. Ostrom Q.T., Gittleman H., Stetson L., Virk S., Barnholtz-Sloan J.S., Epidemiology of Intracranial Gliomas, *Prog Neurol Surg.* 30 (2018) 1-11, <https://doi.org/10.1159/000464374>.
2. Perry J.R., Laperriere N., O'Callaghan C.J., et al., Short-Course Radiation plus Temozolomide in Elderly Patients with Glioblastoma, *N Engl J Med.* 376 (2017) 1027-1037, <https://doi.org/10.1056/NEJMoa1611977>.
3. Van Mieghem E., Wozniak A., Geussens Y., et al., Defining pseudoprogression in glioblastoma multiforme, *Eur J Neurol.* 20 (2013) 1335-1341, <https://doi.org/10.1111/ene.12192>.
4. Abbasi A.W., Westerlaan H.E., Holtman G.A., Aden K.M., van Laar P.J., van der Hoorn A., Incidence of Tumour Progression and Pseudoprogression in High-Grade Gliomas: a Systematic Review and Meta-Analysis, *Clin Neuroradiol.* 28 (2018) 401-411, <https://doi.org/10.1007/s00062-017-0584-x>.
5. Blasel S., Zagorcic A., Jurcoane A., et al., Perfusion MRI in the Evaluation of Suspected Glioblastoma Recurrence, *J Neuroimaging.* 26 (2016) 116-123, <https://doi.org/10.1111/jon.12247>.
6. Khalifa J., Tensaouti F., Chaltiel L., et al., Identification of a candidate biomarker from perfusion MRI to anticipate glioblastoma progression after chemoradiation, *Eur Radiol.* 26 (2016) 4194-4203, <https://doi.org/10.1007/s00330-016-4234-5>.
7. Shiroishi M.S., Castellazzi G., Boxerman J.L., et al., Principles of T2*-weighted dynamic susceptibility contrast MRI technique in brain tumor imaging, *J Magn Reson Imaging.* 41 (2015) 296-313, <https://doi.org/10.1002/jmri.24648>.
8. Patel P., Baradaran H., Delgado D., et al., MR perfusion-weighted imaging in the evaluation of high-grade gliomas after treatment: a systematic review and meta-analysis, *Neuro Oncol.* 19 (2017) 118-127,

- <https://doi.org/10.1093/neuonc/now148>.
9. Jensen J.H., Helpert J.A., Ramani A., Lu H., Kaczynski K., Diffusional kurtosis imaging: the quantification of non-gaussian water diffusion by means of magnetic resonance imaging, *Magn Reson Med.* 53 (2005) 1432-1440, <https://doi.org/10.1002/mrm.20508>.
 10. Falk Delgado A., Nilsson M., van Westen D., Falk Delgado A., Glioma Grade Discrimination with MR Diffusion Kurtosis Imaging: A Meta-Analysis of Diagnostic Accuracy, *Radiology.* 287 (2018) 119-127, <https://doi.org/10.1148/radiol.2017171315>.
 11. Zhao J., Wang Y.L., Li X.B., et al., Comparative analysis of the diffusion kurtosis imaging and diffusion tensor imaging in grading gliomas, predicting tumour cell proliferation and IDH-1 gene mutation status, *J Neurooncol.* 141 (2019) 195-203, <https://doi.org/10.1007/s11060-018-03025-7>.
 12. Tan Y., Zhang H., Wang X., et al., Comparing the value of DKI and DTI in detecting isocitrate dehydrogenase genotype of astrocytomas, *Clin Radiol.* 74 (2019) 314-320, <https://doi.org/10.1016/j.crad.2018.12.004>.
 13. Ion-Mărgineanu A., Van Cauter S., Sima D.M., et al., Classifying Glioblastoma Multiforme Follow-Up Progressive vs. Responsive Forms Using Multi-Parametric MRI Features, *Front Neurosci.* 10 (2016) 615, <https://doi.org/10.3389/fnins.2016.00615>.
 14. Wu X.F., Liang X., Wang X.C., et al., Differentiating high-grade glioma recurrence from pseudoprogression: Comparing diffusion kurtosis imaging and diffusion tensor imaging, *Eur J Radiol.* 135 (2021) 109445, <https://doi.org/10.1016/j.ejrad.2020.109445>.
 15. Tan Y., Wang X.C., Zhang H., et al., Differentiation of high-grade-astrocytomas from solitary-brain-metastases: Comparing diffusion kurtosis imaging and diffusion tensor imaging, *Eur J Radiol.* 84 (2015) 2618-24, <https://doi.org/10.1016/j.ejrad.2015.10.007>.
 16. Calamante F., Arterial input function in perfusion MRI: a comprehensive review,

- Prog Nucl Magn Reson Spectrosc. 74 (2013) 1-32,
<https://doi.org/10.1016/j.pnmrs.2013.04.002>.
17. Mahase S., Rattenni R.N., Wesseling P., et al., Hypoxia-Mediated Mechanisms Associated with Antiangiogenic Treatment Resistance in Glioblastomas, *Am J Pathol.* 187 (2017) 940-953, <https://doi.org/10.1016/j.ajpath.2017.01.010>.
18. Wu E.X., Cheung M.M., MR diffusion kurtosis imaging for neural tissue Characterization, *NMR Biomed.* 23(2010)836-848,
<https://doi.org/10.1002/nbm.1506>.
19. Wang S., Martinez-Lage M., Sakai Y., et al., Differentiating Tumor Progression from Pseudoprogression in Patients with Glioblastomas Using Diffusion Tensor Imaging and Dynamic Susceptibility Contrast MRI, *AJNR Am J Neuroradiol.* 37 (2016) 28-36, <https://doi.org/10.3174/ajnr.A4474>.
20. Agarwal A., Kumar S., Narang J., et al., Morphologic MRI features, diffusion tensor imaging and radiation dosimetric analysis to differentiate pseudo-progression from early tumor progression, *J Neurooncol.* 112 (2013) 413-420,
<https://doi.org/10.1007/s11060-013-1070-1>.
21. Li H., Li J., Cheng G., Zhang J., Li X., IDH mutation and MGMT promoter methylation are associated with the pseudoprogression and improved prognosis of glioblastoma multiforme patients who have undergone concurrent and adjuvant temozolomide-based chemoradiotherapy, *Clin Neurol Neurosurg.* 151 (2016) 31-36, <https://doi.org/10.1016/j.clineuro.2016.10.004>.
22. Barajas R.F. Jr., Chang J.S., Segal M.R., et al., Differentiation of recurrent glioblastoma multiforme from radiation necrosis after external beam radiation therapy with dynamic susceptibility-weighted contrast-enhanced perfusion MR imaging, *Radiology.* 253 (2009) 486-496,
<https://doi.org/10.1148/radiol.2532090007>.
23. Yun T.J., Park C.K., Kim T.M., et al., Glioblastoma treated with concurrent radiation therapy and temozolomide chemotherapy: differentiation of true

- progression from pseudoprogression with quantitative dynamic contrast-enhanced MR imaging, *Radiology*. 274 (2015) 830-40, <https://doi.org/10.1148/radiol.14132632>.
24. Kong Z., Yan C., Zhu R., et al., Imaging biomarkers guided anti-angiogenic therapy for malignant gliomas, *Neuroimage Clin*. 20 (2018) 51-60, <https://doi.org/10.1016/j.nicl.2018.07.001>.
25. Ellingson B.M., Wen P.Y., Cloughesy T.F., Modified Criteria for Radiographic Response Assessment in Glioblastoma Clinical Trials, *Neurotherapeutics*. 14 (2017) 307-320, <https://doi.org/10.1007/s13311-016-0507-6>.
26. Suh C.H., Kim H.S., Jung S.C., Choi C.G., Kim S.J., Multiparametric MRI as a potential surrogate endpoint for decision-making in early treatment response following concurrent chemoradiotherapy in patients with newly diagnosed glioblastoma: a systematic review and meta-analysis, *Eur Radiol*. 28 (2018) 2628-2638, <https://doi.org/10.1007/s00330-017-5262-5>.
27. Kim J.Y., Park J.E., Jo Y., et al., Incorporating diffusion- and perfusion-weighted MRI into a radiomics model improves diagnostic performance for pseudoprogression in glioblastoma patients, *Neuro Oncol*. 21 (2019) 404-414, <https://doi.org/10.1093/neuonc/noy133>.
28. Prager A.J., Martinez N., Beal K., Omuro A., Zhang Z., Young R.J., Diffusion and perfusion MRI to differentiate treatment-related changes including pseudoprogression from recurrent tumors in high-grade gliomas with histopathologic evidence, *AJNR Am J Neuroradiol*. 36 (2015) 877-85, <https://doi.org/10.3174/ajnr.A4218>.
29. Chakhoyan A., Woodworth D.C., Harris R.J., et al., Mono-exponential, diffusion kurtosis and stretched exponential diffusion MR imaging response to chemoradiation in newly diagnosed glioblastoma, *J Neurooncol*. 139 (2018) 651-659, <https://doi.org/10.1007/s11060-018-2910-9>.

Tables

Table 1. Clinical characteristics of patients with glioma recurrence or

pseudoprogression

Table 2. DKI, DSC and DWI parameters of glioma recurrence and pseudoprogression

Table 3. Receiver operating curve analysis of DKI, DSC and DWI parameters in differentiating glioma recurrence from pseudoprogression

Figure legends

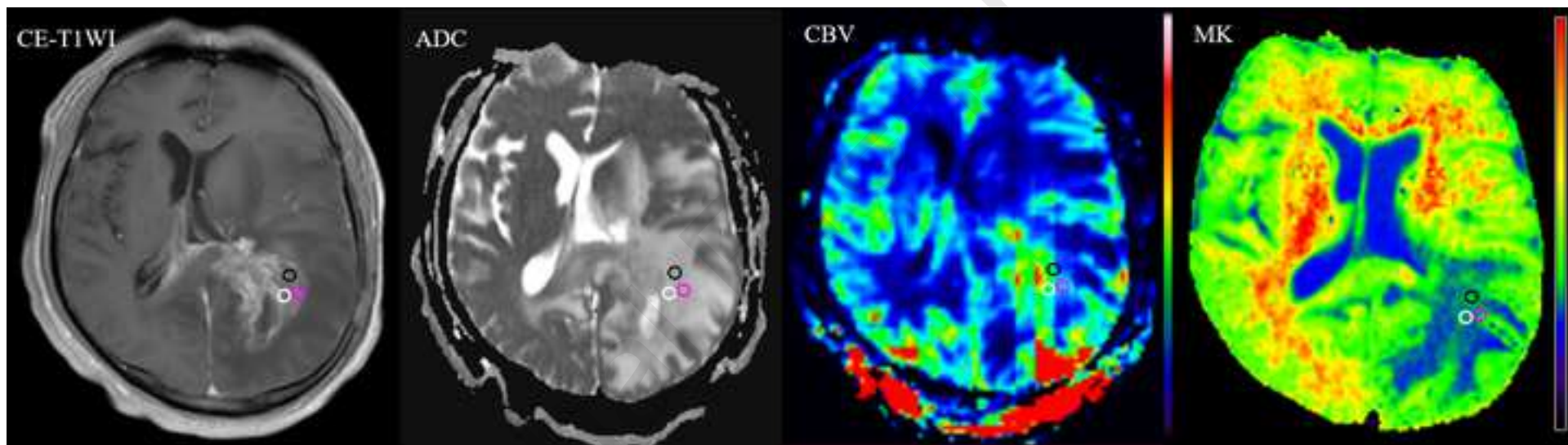
Figure 1: Placement of ROIs. A 50-year-old male developed pseudoprogression after treated glioma.

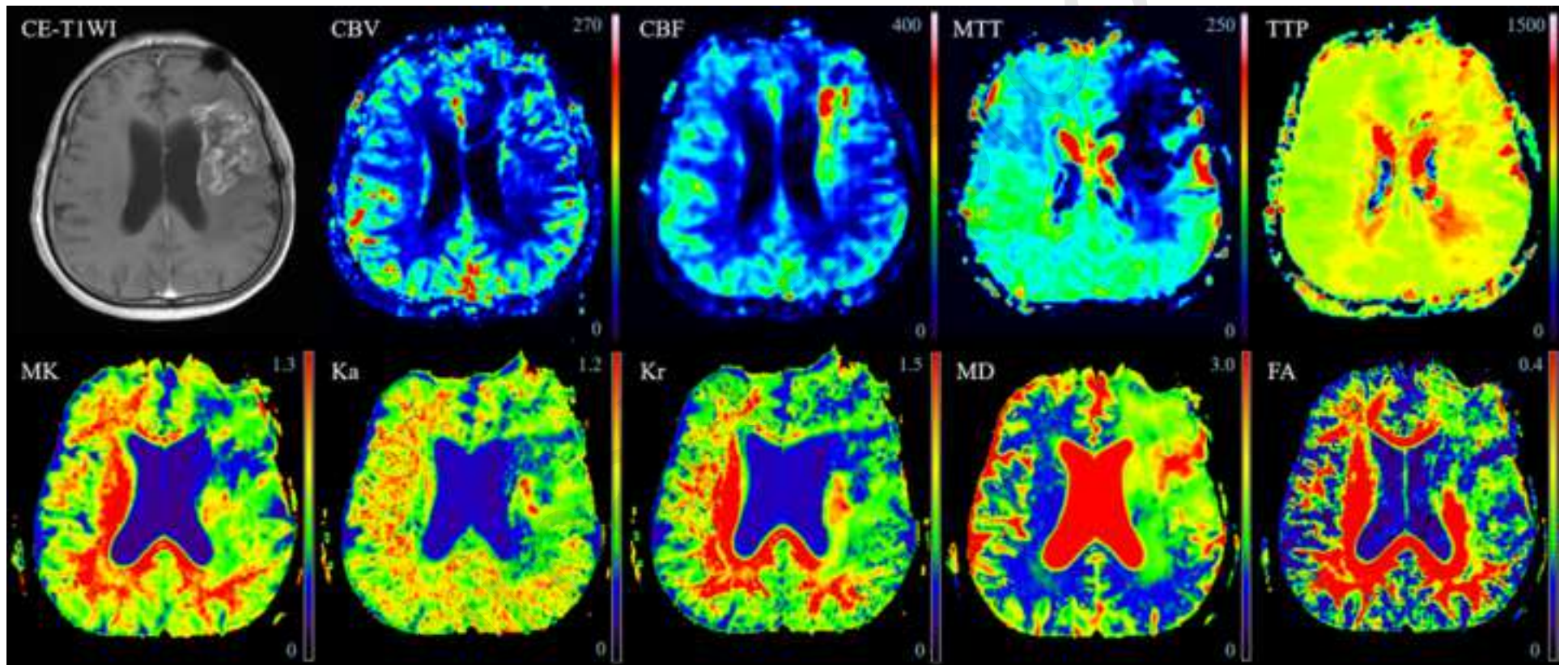
Figure 2. A 70-year-old man with treated glioblastoma was biopsied to be a pseudoprogression. A newly enhancing lesion in the left frontal and temporal lobes was detected on CE-T1WI with decreased CBV, MTT, MK, Ka, Kr and FA values, except for CBF, TTP and MD values.

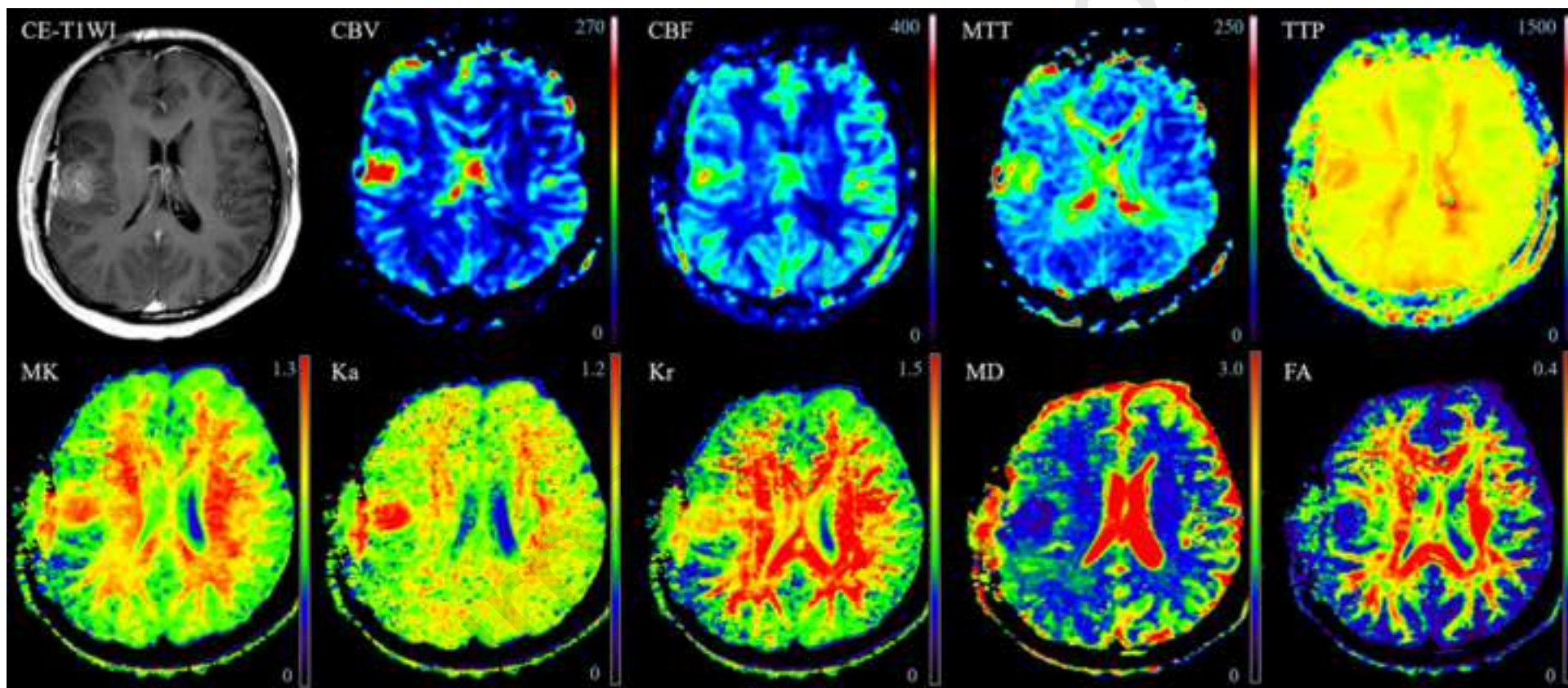
Figure 3. A 21-year-old man with tumor recurrence confirmed by repeat surgery was initially a glioblastoma. An increasing enhanced lesion in the right frontal and temporal lobes was detected on CE-T1WI with increased CBV, CBF, MTT, TTP, MK, Ka and Kr values, except for MD and FA values.

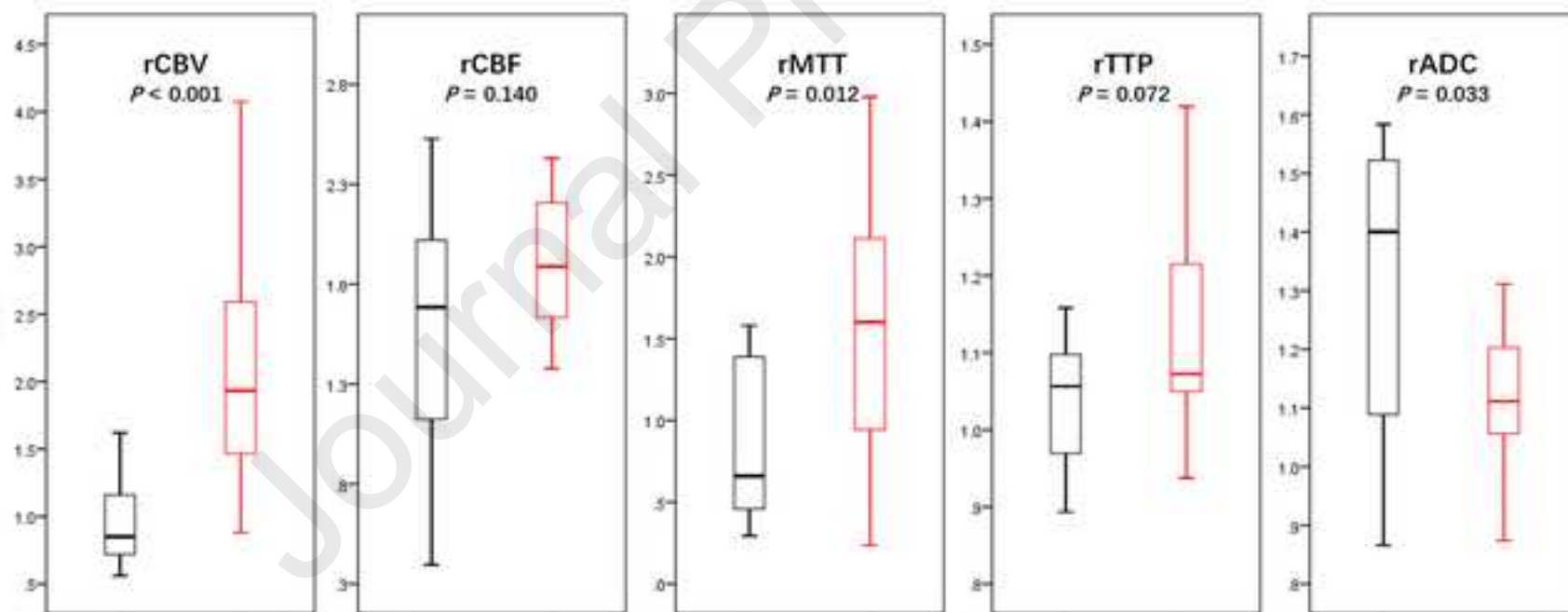
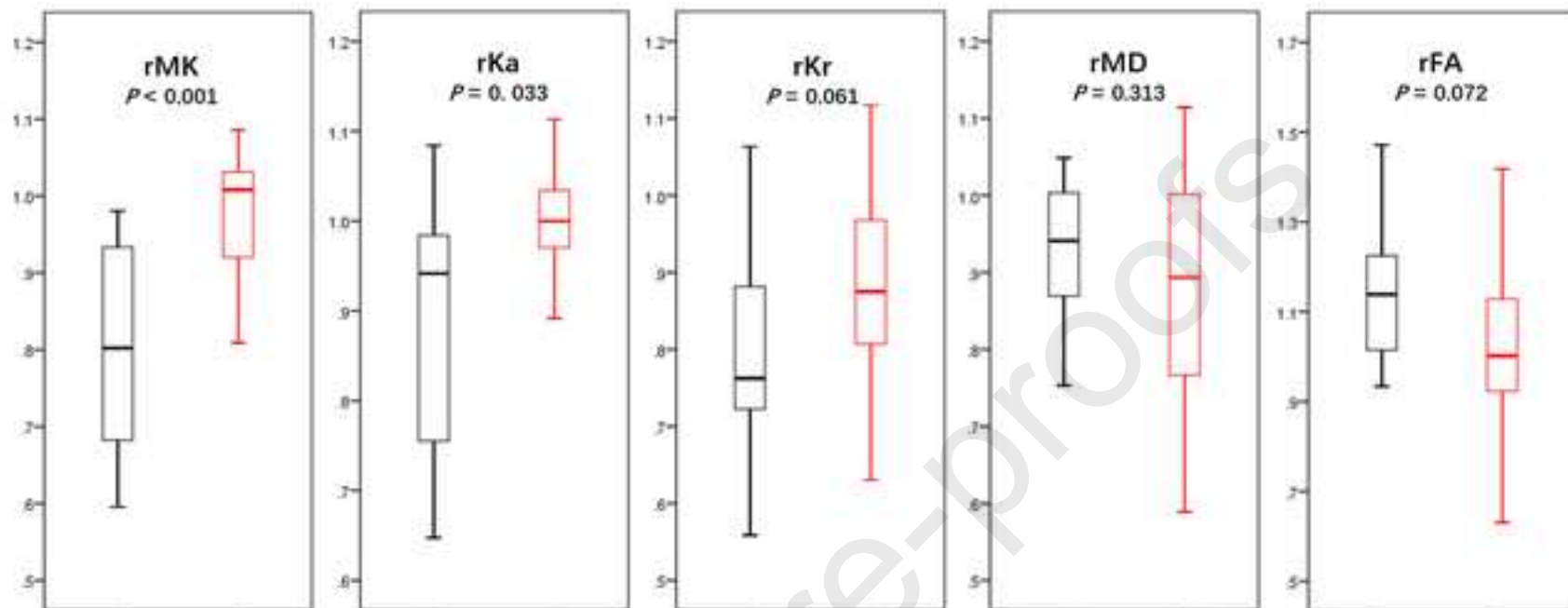
Figure 4. The box-and-whiskers graphs for the DKI, DSC and DWI parameters.

Figure 5. ROC curves of DKI, DSC and DWI parameters for differentiating glioma recurrence from pseudoprogression. A, ROC curves of rMK, rCBV, and the combine. B, ROC curves of rKa, rMTT and rADC. Combine = rMK + rCBV.









Pseudoproggression
 Recurrence

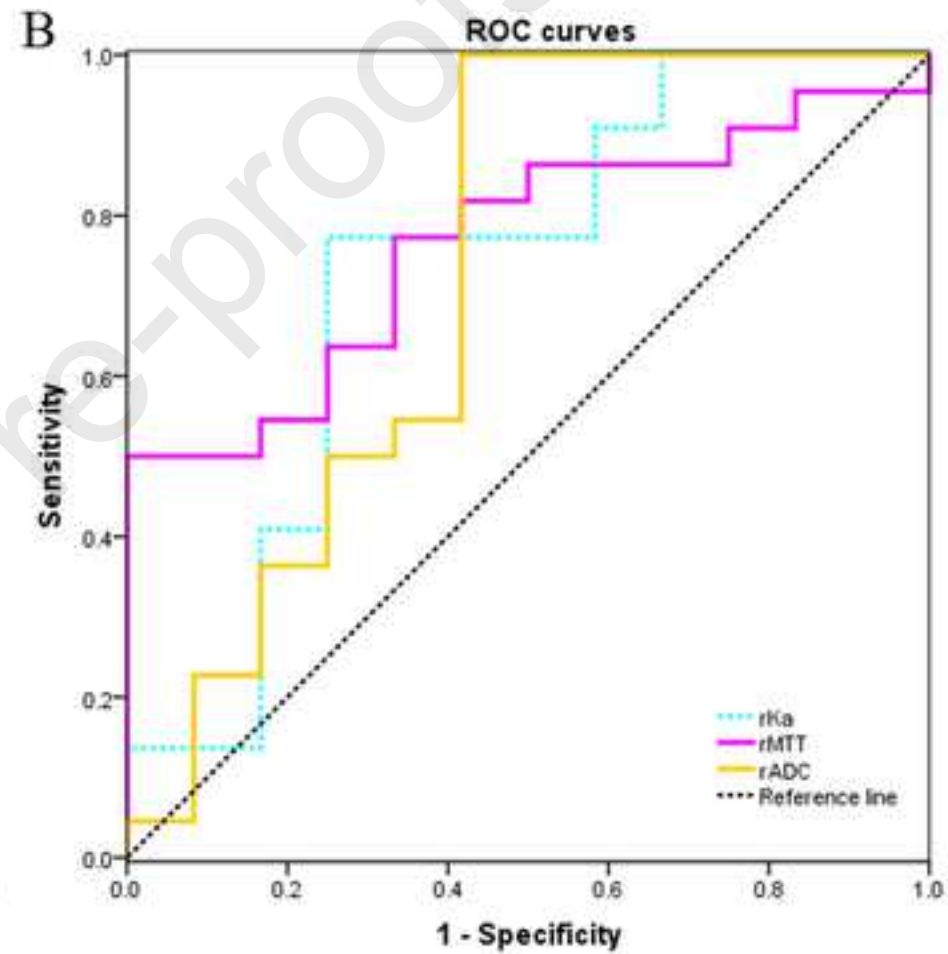
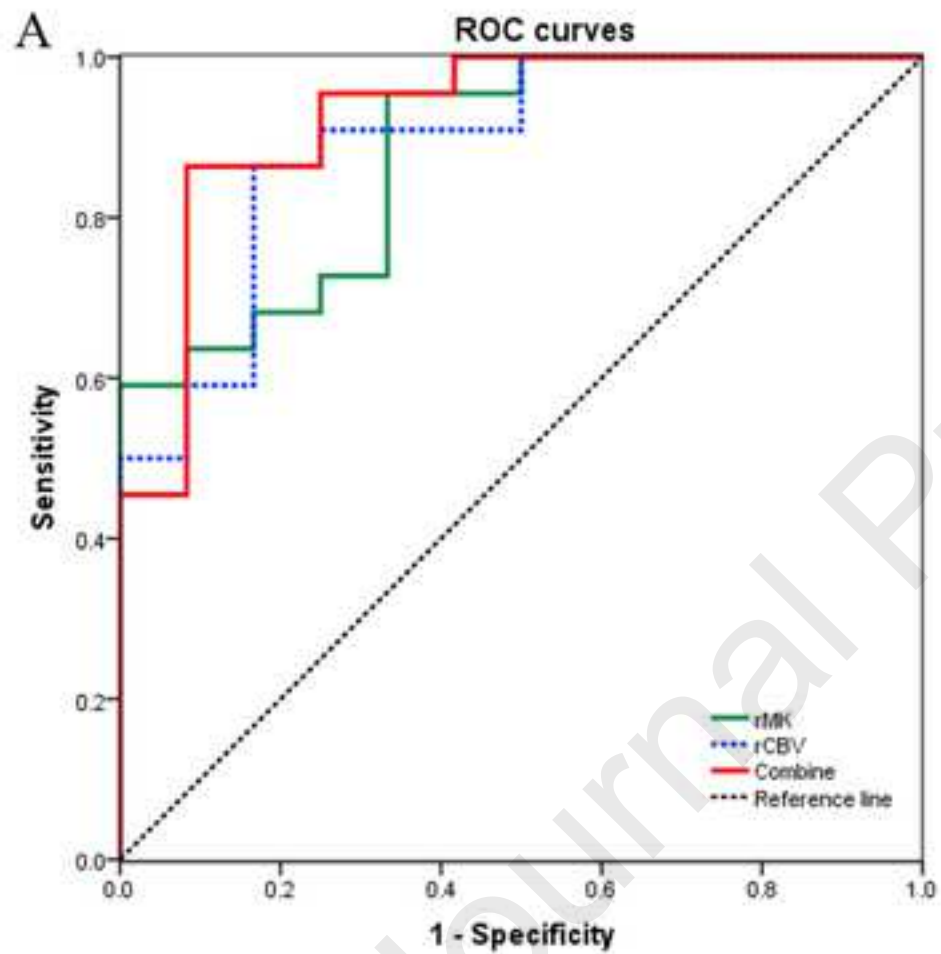


Table 1. Clinical characteristics of patients with glioma recurrence or pseudoprogression

Characteristics	Total (n = 34)	Recurren ce (n = 22)	Pseudoprogre ssion (n = 12)	P value
Sex (n)				0.502
Male	24 (70.6%)	16 (72.7%)	8 (66.7%)	
Female	10 (29.4%)	6 (27.3%)	4 (33.3%)	
Age (years)				0.607
Mean ± SD	47 ± 14.07	44 ± 13.18	51 ± 15.10	
Range	21-70	21-64	23-70	
Grade (n)				0.439
WHO III	15 (44.1%)	9 (40.9%)	6 (50%)	
WHO IV	19 (55.9%)	13 (59.1%)	6 (50%)	
IDH status (n)	27	17	10	0.089
Mutant	13 (48.1%)	6 (35.3%)	7 (70%)	
Wild	14 (51.9%)	11 (64.7%)	3 (30%)	
KPS score (n)				0.297
≥ 60	25 (73.5%)	15 (68.2%)	10 (83.3%)	

< 60	9 (26.5%)	7 (31.8%)	2 (16.7%)	
Radiation Dose				0.332
(Gy)				
Median	60	60	60	
Range	50-64.2	54-60	50-64.2	

SD, standard deviation; IDH, isocitrate dehydrogenase; KPS, Karnofsky Performance Status.

Table 2. DKI, DSC and DWI parameters of glioma recurrence and pseudoprogression

Parameters	Recurrence (<i>n</i> = 22)	Pseudoprogression (<i>n</i> = 12)	<i>P</i> value
D			<
KI			0.001
rMK	1.01 (0.81, 1.09)	0.80 (0.60, 0.98)	0.03
rKa	1.00 (0.77, 1.14)	0.94 (0.65, 1.08)	3
rKr	0.88 (0.63, 1.12)	0.76 (0.56, 1.06)	0.06
rMD	0.89 (0.59, 1.11)	0.94 (0.75, 1.25)	1
			0.31

				3
	rFA	1.00 (0.55, 1.75)	1.14 (0.93, 2.04)	0.07
				2
D	rCBV	1.93 (0.88, 4.08)	0.85 (0.56, 2.08)	<
SC				0.001
	rCBF	1.89 (1.38, 3.84)	1.68 (0.45, 2.12)	0.14
				0
	rMTT	1.60 (0.24, 2.98)	0.66 (0.30, 1.58)	0.01
				2
	rTTP	1.07 (0.94, 1.41)	1.06 (0.75, 1.14)	0.07
				2
D	rADC	1.09 (0.76, 1.29)	1.38 (0.85, 1.56)	0.03
WI				3

rMK, relative mean kurtosis; rKa, relative axial kurtosis; rKr, relative radial kurtosis; rMD, relative mean diffusivity; rFA, relative fractional anisotropy; rCBV, relative cerebral blood volume; rCBF, relative cerebral blood flow; rMTT, relative mean transit time; rTTP, relative time to peak; rADC, relative apparent diffusion coefficient.

Table 3. Receiver operating curve analysis of DKI, DSC and DWI parameters in

differentiating glioma recurrence from pseudoprogression

Paramet ers	AUC (95%CI)	Cut-off value	Accu racy (%)	Sensi tivity (%)	Speci ficity (%)	P value
rMK	0.879 (0.721, 0.965)	0.889	82.35	95.45	66.67	< 0.001
rKa	0.723 (0.544, 0.862)	0.960	70.59	77.27	75	0. 030
rCBV	0.890 (0.735, 0.971)	1.348	82.35	86.36	83.33	< 0.001
rMTT	0.765 (0.589, 0.893)	1.276	73.53	63.64	75	0. 001
rADC	0.723 (0.544, 0.862)	1.292	82.35	100	58.33	0. 041
Combine	0.924 (0.780, 0.987)	-	88.24	86.36	91.67	< 0.001

AUC, area under the curve; CI, confidence interval; rMK, relative mean kurtosis; rKa, relative axial kurtosis; rCBV, relative cerebral blood volume; rMTT, relative mean transit time; rADC, relative apparent diffusion coefficient; Combine = rMK + rCBV.

The authors declared that they have no conflicts of interest to this work.

Journal Pre-proofs

Wenwei Shi: Supervision, Writing - original draft, Writing - review & editing.
Chongxiao Qu: Supervision, Writing - original draft, Writing - review & editing.
Xiaochun Wang: Formal analysis, Funding acquisition. **Xiao Liang:** Data curation, Software. **Yan Tan:** Conceptualization, Funding acquisition, Project administration.
Hui Zhang: Conceptualization, Funding acquisition, Project administration.

Journal Pre-proofs

Highlights

- *Diffusion kurtosis imaging (DKI) is a potential non-invasive imaging biomarker of response that may help differentiate glioma recurrence from pseudoprogression.*
- *DKI and dynamic susceptibility contrast-enhanced (DSC) MRI may have a complementary predictive value for the discrimination.*
- *The combined use of DKI and DSC MRI can improve the diagnostic performance in assessing treatment response than either technique alone.*